



ISTITUTO NAZIONALE DI RICERCA METROLOGICA Repository Istituzionale

Heteroclinic tangle phenomena in nanomagnets subject to time-harmonic excitations

Original

Heteroclinic tangle phenomena in nanomagnets subject to time-harmonic excitations / Serpico, C.; Quercia, A.; Bertotti, G.; D'Aquino, M.; Mayergoyz, I.; Perna, S.; Ansalone, P.. - In: JOURNAL OF APPLIED PHYSICS. - ISSN 1089-7550. - 117:17(2015). [10.1063/1.4914530]

Availability:

This version is available at: 11696/65540 since: 2021-03-09T22:09:51Z

Publisher:

AIP Publishing LLC

Published

DOI:10.1063/1.4914530

Terms of use:

This article is made available under terms and conditions as specified in the corresponding bibliographic description in the repository

Publisher copyright

(Article begins on next page)

Heteroclinic tangle phenomena in nanomagnets subject to time-harmonic excitations

C. Serpico, A. Quercia, G. Bertotti, M. d'Aquino, I. Mayergoyz, S. Perna, and P. Ansalone

Citation: *Journal of Applied Physics* **117**, 17B719 (2015); doi: 10.1063/1.4914530

View online: <http://dx.doi.org/10.1063/1.4914530>

View Table of Contents: <http://scitation.aip.org/content/aip/journal/jap/117/17?ver=pdfcov>

Published by the [AIP Publishing](#)

Articles you may be interested in

Reply to "Comment on 'Metastable state in a shape-anisotropic single-domain nanomagnet subjected to spin-transfer torque'" [*Appl. Phys. Lett.* **105**, 116101 (2014)]

Appl. Phys. Lett. **105**, 116103 (2014); 10.1063/1.4894642

Comment on "Metastable state in a shape-anisotropic single-domain nanomagnet subjected to spin-transfer-torque" [*Appl. Phys. Lett.* **101**, 162405 (2012)]

Appl. Phys. Lett. **105**, 116101 (2014); 10.1063/1.4894640

Stochastic bifurcation and fractal and chaos control of a giant magnetostrictive film-shape memory alloy composite cantilever plate subjected to in-plane harmonic and stochastic excitation

J. Appl. Phys. **115**, 17E527 (2014); 10.1063/1.4868182

Melnikov's criteria, parametric control of chaos, and stationary chaos occurrence in systems with asymmetric potential subjected to multiscale type excitation

Chaos **21**, 043113 (2011); 10.1063/1.3650699

Chaotic dynamics of the nuclear magnetization on account of resonator effects

Low Temp. Phys. **32**, 915 (2006); 10.1063/1.2364479



You don't still use this cell phone

or this computer

Why are you still using an AFM designed in the 80's?

It is time to upgrade your AFM

Minimum \$20,000 trade-in discount for purchases before August 31st

Asylum Research is today's technology leader in AFM

dropmyoldAFM@oxinst.com

OXFORD
INSTRUMENTS
The Business of Science®

Heteroclinic tangle phenomena in nanomagnets subject to time-harmonic excitations

C. Serpico,^{1,a)} A. Quercia,¹ G. Bertotti,² M. d'Aquino,³ I. Mayergoyz,⁴ S. Perna,¹ and P. Ansalone²

¹DIETI, Università di Napoli "Federico II," I-80125 Napoli, Italy

²Istituto Nazionale di Ricerca Metrologica, I-10135 Torino, Italy

³Dip. di Ingegneria, Università di Napoli "Parthenope," I-80143 Napoli, Italy

⁴ECE Department and UMIACS, University of Maryland, College Park, Maryland 20742, USA

(Presented 7 November 2014; received 22 September 2014; accepted 31 October 2014; published online 20 March 2015)

Magnetization dynamics in uniformly magnetized nanomagnets excited by time-harmonic (AC) external fields or spin-polarized injected currents is considered. The analysis is focused on the behaviour of the AC-excited dynamics near saddle equilibria. It turns out that this dynamics has a chaotic character at moderately low power level. This chaotic and fractal nature is due to the phenomenon of heteroclinic tangle which is produced by the combined effect of AC-excitations and saddle type dynamics. By using the perturbation technique based on Melnikov function, analytical formulas for the threshold AC excitation amplitudes necessary to create the heteroclinic tangle are derived. Both the cases of AC applied fields and AC spin-polarized injected currents are treated. Then, by means of numerical simulations, we show how heteroclinic tangle is accompanied by the erosion of the safe basin around the stable regimes. © 2015 AIP Publishing LLC.

[<http://dx.doi.org/10.1063/1.4914530>]

Magnetization dynamics in uniformly magnetized ferromagnets driven by time-harmonic (AC) excitations has been extensively studied in connection with the phenomenon of ferromagnetic resonance.¹ In this case, AC fields produce small magnetization oscillations around a stable equilibrium. The response of the system depends on the frequency of the excitation and, in the linear regime, follows the usual resonance curve peaked around the Kittel frequency.² Owing to the weakly dissipative nature of magnetization dynamics, nonlinear effects are excited at moderately large powers, at which the resonance response may become hysteretic (bistable) due the fold-over effect.³

In this paper, we study a similar problem but we want to investigate the effects of time-harmonic excitations in a wider region of the state space. More specifically, we are interested in the regions around saddle-type equilibria which are usually at the top of the potential wells. The reason for studying such an unstable region is related to the fact that saddle equilibria and the associated heteroclinic/homoclinic manifolds connecting the saddles, which are referred to as homoclinic/heteroclinic cycles, constitute the separatrices, namely, the boundaries of basins of attraction of different attractors (asymptotic regimes). It turns out that the AC perturbations of the dynamics in the vicinity of saddle equilibria give rise to phenomena incomparably more complex of those observed in the vicinity of a stable equilibrium.

These complex phenomena are due to the possibility that the homoclinic/heteroclinic manifolds, at sufficiently large AC excitations, may intersect infinitely many times forming a structure referred to as homoclinic/heteroclinic tangle which

may lead to separatrices which have a fractal geometrical nature. One of the main consequences of these phenomena is that the magnetization motions starting inside an energy well may, at later time, escape the well. This mechanism is called basin erosion and it starts in the vicinity of the saddle equilibria and the associated homoclinic/heteroclinic cycles.⁴

The aim of this paper is to bring attention on the phenomena above introduced which, in the area of applied magnetism, have been largely overlooked. In the paper, magnetization dynamics is described by the Landau-Lifshitz (LL) equation appropriately generalized to take into account the effect of spin polarized currents. The external excitation conditions are taken to be purely sinusoidal with zero bias in both the applied fields and the injected currents. In these conditions, the entanglement of saddle manifolds is of the heteroclinic type. The origin of heteroclinic tangle is first illustrated from the qualitative point of view. Then, by using the perturbation techniques based on Melnikov function,⁵ we derive analytical formulas for the threshold values of AC applied fields and of AC injected spin-polarized currents for the onset of the heteroclinic tangle. In the final part of the paper, we discuss the phenomenon of basin erosion on the basis of numerical simulations.

The evolution of the magnetization \mathbf{M} in a uniformly magnetized ferromagnet is described in terms of normalized vector $\mathbf{m} = \mathbf{M}/M_s$, where M_s is the saturation magnetization and $|\mathbf{m}| = 1$. The evolution of \mathbf{m} on the unit sphere Σ is governed by the following generalized Landau-Lifshitz equation⁶

$$\frac{d\mathbf{m}}{dt} = \mathbf{m} \times \nabla_{\Sigma} g - \nabla_{\Sigma} \psi, \quad (1)$$

where ∇_{Σ} is the gradient operator on the unit sphere, $g = g(\mathbf{m}, t)$ is the free energy, and $\psi = \psi(\mathbf{m}, t)$ is a potential

^{a)}Author to whom correspondence should be addressed. Electronic mail: serpico@unina.it.

function which takes into account effects of damping and spin-torque. We use normalized quantities so that time is measured in units of $(\gamma M_s)^{-1}$, where γ is the gyromagnetic ratio, and the energy functions g and ψ in units of $\mu_0 M_s^2 V$, where μ_0 is the vacuum permeability and V is the volume of the particle. The free energy is given by the following expression:

$$g(\mathbf{m}, t) = g_0(\mathbf{m}) - \mathbf{h}_{ac}(t) \cdot \mathbf{m}, \quad (2)$$

where

$$g_0(\mathbf{m}) = (D_x m_x^2 + D_y m_y^2 + D_z m_z^2)/2, \quad (3)$$

where D_x , D_y , and D_z are effective anisotropy constants. The field $\mathbf{h}_{ac}(t)$ in Eq. (2) is the time-harmonic (AC) external field

$$\begin{aligned} \mathbf{h}_{ac}(t) = & \mathbf{e}_x h_{ax} \cos(\omega t + \delta_x) + \mathbf{e}_y h_{ay} \cos(\omega t + \delta_y) \\ & + \mathbf{e}_z h_{az} \cos(\omega t + \delta_z), \end{aligned} \quad (4)$$

where \mathbf{e}_x , \mathbf{e}_y , and \mathbf{e}_z are the cartesian unit vectors, and where h_{ax} , h_{ay} , h_{az} , δ_x , δ_y , and δ_z are the amplitudes and phases of the cartesian components of $\mathbf{h}_{ac}(t)$, respectively. In addition, we assume

$$\psi(\mathbf{m}, t) = \alpha g(\mathbf{m}, t) + \beta(t)(\mathbf{m} \cdot \mathbf{e}_p), \quad (5)$$

where the first term at the right-hand-side is the usual Landau-Lifshitz damping term (α is the damping constant), while the second term takes into account the spin-torque effect.⁶ The quantity

$$\beta(t) = \beta_{ac} \cos(\omega t + \delta_p) \quad (6)$$

is the AC normalized spin-polarized current and \mathbf{e}_p is the electron polarization orientation.

In most cases of practical and physical interest, it happens that α , h_{ac} , $\beta_{ac} \ll 1$ ($h_{ac} = \sqrt{h_{ax}^2 + h_{ay}^2 + h_{az}^2}$). This leads to the following perturbative form of Eq. (1):

$$\frac{d\mathbf{m}}{dt} = \mathbf{v}_0(\mathbf{m}) + \varepsilon \mathbf{v}_1(\mathbf{m}, t) = \mathbf{v}(\mathbf{m}, t, \varepsilon), \quad (7)$$

where $\mathbf{v}_0(\mathbf{m}) = \mathbf{m} \times \nabla_{\Sigma} g_0(\mathbf{m})$ is the unperturbed hamiltonian vector field and $\varepsilon \mathbf{v}_1(\mathbf{m}, t) = -\mathbf{m} \times \mathbf{h}_{ac}(t) - \nabla_{\Sigma} \psi(\mathbf{m}, t)$. The parameter ε is formally introduced in preparation of a perturbation analysis of the dynamics based on the assumption that $\varepsilon \ll 1$. One can interpret ε as a parameter which controls the amplitude of all small quantities in the problem, and more specifically, the amplitude of AC excitations. In the form (7), the equation governing magnetization dynamics is a perturbed hamiltonian dynamics on the unit sphere with hamiltonian given by the function $g_0(\mathbf{m})$.

The non-autonomous dynamical system (7) can be analyzed by introducing the stroboscopic map⁷

$$\mathbf{m}_{n+1} = P[\mathbf{m}_n, \varepsilon], \quad (8)$$

where $\mathbf{m}_n = \mathbf{m}(t_0 + nT)$ and $T = 2\pi/\omega$, which maps an initial magnetization $\mathbf{m}(t_0)$ to the magnetization $\mathbf{m}(t_0 + T)$

obtained by integrating Eq. (7), over a time interval equal to T . Notice that the stroboscopic map (8) is a time-discrete dynamical system and thus its trajectories are sequence of points on Σ . In order to develop an analytical treatment of $P[\cdot]$, we consider the following Taylor expansion:

$$P[\mathbf{m}_n, \varepsilon] = P[\mathbf{m}_n, 0] + \frac{\partial P}{\partial \varepsilon}[\mathbf{m}_n, 0]\varepsilon + \mathcal{O}(\varepsilon^2). \quad (9)$$

The zero order term of the expansion gives the unperturbed map the trajectories which lie on the curves with constant value of $g_0(\mathbf{m})$ and these can be determined in closed form.⁶ This implies that the unperturbed map $P[\mathbf{m}_n, 0]$ admits, as saddle fixed points, the saddle equilibria associated with the vector field $\mathbf{v}_0(\mathbf{m})$. The qualitative features of the phase portrait of $\mathbf{v}_0(\mathbf{m})$ in cylindrical coordinate (ϕ, m_z) are sketched in Fig. 1(a). The two saddles \mathbf{x}_{d1} and \mathbf{x}_{d2} are connected through heteroclinic trajectories, which are invariant set of the map $P[\mathbf{m}_n, 0]$. We recall that an invariant set A of a map $P[\cdot]$ is such that $P[A] \subseteq A$. Heteroclinic trajectories are typical only in conservative systems and they are not structurally stable with respect to generic perturbation of the system. For this reason, they are immediately destroyed when nonconservative perturbations set in. On the other hand, saddle fixed

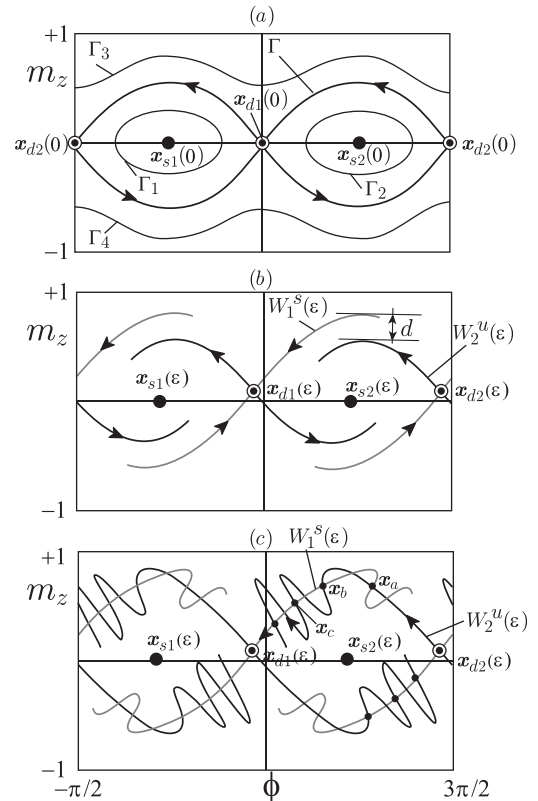


FIG. 1. Qualitative sketches of the separatrices associated to the stroboscopic map (see Eq. (8)) in the (ϕ, m_z) -plane (where ϕ is the azimuth around the z -axis). (a) Unperturbed case; (b) damping dominated dynamics; (c) heteroclinic tangle formation. Legend: $\mathbf{x}_{d1}(\varepsilon)$, $\mathbf{x}_{d2}(\varepsilon)$ are the saddle equilibria; $\mathbf{x}_{s1}(\varepsilon)$, $\mathbf{x}_{s2}(\varepsilon)$ are the node-type equilibria; $W_1^s(\varepsilon)$ is the stable manifold associated with $\mathbf{x}_{d1}(\varepsilon)$; $W_2^u(\varepsilon)$ is the unstable manifold associated with $\mathbf{x}_{d2}(\varepsilon)$; d is the splitting of the manifolds; Γ is the heteroclinic trajectory, and Γ_1 - Γ_4 are the constant energy trajectories. The points \mathbf{x}_a , \mathbf{x}_b , \mathbf{x}_c are generated by iterating the stroboscopic map.

points are structurally stable entities⁸ and thus are preserved under small perturbations. In the perturbed case, from each saddle of the map, two invariant curves arise: the stable manifold W^s and the unstable manifold W^u .^{7,8} In Fig. 1(b), the two manifolds $W_1^s(\varepsilon)$ and $W_2^u(\varepsilon)$ are sketched and their separation (splitting) is indicated by d . This splitting depends on the nature of perturbation and for sufficiently large AC perturbations it may vanish. When this is the case, a point of intersection \mathbf{x}_a belonging to both invariant sets $W_1^s(\varepsilon)$ and $W_2^u(\varepsilon)$ is realized (see Fig. 1(c)). This implies that forward and backward iterates of $P[\cdot]$ starting from \mathbf{x}_a must belong to $W_1^s(\varepsilon) \cap W_2^u(\varepsilon)$ and thus that the two curves $W_1^s(\varepsilon)$, $W_2^u(\varepsilon)$, must intersect an infinite number of times (see Fig. 1(c)). This phenomenon is referred to as heteroclinic tangle and it is at the origin of chaotic and unpredictable dynamic behaviour of the system near the saddles. In order to find when this occurs, one must be able to compute the splitting d of $W_1^s(\varepsilon)$ and $W_2^u(\varepsilon)$. It turns out that, by using the expansion (8), the splitting can be derived analytically and it is proportional to the Melnikov function⁸ which we discuss below.

The Melnikov function approach to determine the onset of heteroclinic tangle is based on the availability of analytical expressions⁶ for the unperturbed heteroclinic trajectories

$$\begin{aligned} m_{dx} &= s_x k / \cosh \Omega_d t, \\ m_{dy} &= -s_x s_z \tanh \Omega_d t, \\ m_{dz} &= s_z k' / \cosh \Omega_d t, \end{aligned} \quad (10)$$

where $k^2 = (D_z - D_y)/(D_z - D_x)$, $k'^2 = 1 - k^2$, $\Omega_d = \sqrt{(D_z - D_y)(D_y - D_x)}$ and the combinations of the signs $s_x, s_z = \pm 1$ provide the four heteroclinic trajectories (see Fig. 1(a)). The separatrices are trajectories with constant energy $g_0 = D_y/2$. Thus, by using the expression $\nabla_{\Sigma} f = \nabla f - (\nabla f \cdot \mathbf{m})\mathbf{m}$, we get

$$\nabla_{\Sigma} g_0(\mathbf{m}_d) = \Omega_d \mathbf{e}_{d\uparrow} / \cosh \Omega_d t, \quad (11)$$

where $\mathbf{e}_{d\uparrow} = -s_x k' \mathbf{e}_x + s_z k \mathbf{e}_z$ is a unit normal to the plane containing the great circle given by Eq. (10). The Melnikov function $M(\omega, t_0)$ is given by

$$\begin{aligned} \varepsilon M(\omega, t_0) &= \int_{-\infty}^{+\infty} [\mathbf{m} \cdot \mathbf{v}_0(\mathbf{m}) \times \varepsilon \mathbf{v}_1(\mathbf{m}, t)]_{\mathbf{m}_d(t-t_0)} dt \\ &= \alpha M_0 + h_{ac} M_h(\omega, t_0) + \beta_{ac} M_I(\omega, t_0), \end{aligned}$$

where $M_0 = \int_{-\infty}^{+\infty} |\nabla_{\Sigma} g_0(\mathbf{m}_d(t))|^2 dt = 2\Omega_d$ and

$$h_{ac} M_h(\omega, t_0) = - \int_{-\infty}^{+\infty} \mathbf{h}_{ac}(t+t_0) \cdot \frac{d\mathbf{m}_d(t)}{dt} dt, \quad (12)$$

$$\beta_{ac} M_I(\omega, t_0) = \int_{-\infty}^{+\infty} \beta(t+t_0) \mathbf{e}_p \cdot \nabla_{\Sigma} g_0(\mathbf{m}_d(t)) dt. \quad (13)$$

When the system is driven by the field \mathbf{h}_{ac} alone, i.e., $\beta_{ac} = 0$, the following result holds:

$$\varepsilon M(\omega, t_0) = 2\alpha\Omega_d + |\tilde{\mathbf{h}}_{ac} \cdot \mathbf{u}^*(\omega)| \cos(\omega t_0 + \psi), \quad (14)$$

where $\psi = \angle(\tilde{\mathbf{h}}_{ac} \cdot \mathbf{u}^*)$ and we have set

$$\begin{aligned} \mathbf{h}_{ac}(t) &= \text{Re}\{\tilde{\mathbf{h}}_{ac} e^{i\omega t}\}, \\ \tilde{\mathbf{h}}_{ac} &= h_x e^{i\delta_x} \mathbf{e}_x + h_y e^{i\delta_y} \mathbf{e}_y + h_z e^{i\delta_z} \mathbf{e}_z, \\ \mathbf{u}(\omega) &= (s_x k \mathbf{e}_x + s_z k' \mathbf{e}_z) \frac{-i\pi q}{\cosh \frac{\pi q}{2}} + s_x s_z \mathbf{e}_z \frac{\pi q}{\sinh \frac{\pi q}{2}}. \end{aligned} \quad (15)$$

with $q = \omega/\Omega_d$.

The maximum value of the amplitude of the sinusoidal component of $\varepsilon M(\omega, t_0)$ is achieved when the equal sign of the Schwartz inequality $|\tilde{\mathbf{h}}_{ac} \cdot \mathbf{u}^*| \leq |\tilde{\mathbf{h}}_{ac}| |\mathbf{u}|$ holds, namely, for $\tilde{\mathbf{h}}_{ac} = h_{ac} e^{i\delta} \mathbf{u}/|\mathbf{u}|$.

The threshold values for the onset of the heteroclinic tangle can be found from the zeros of the Melnikov function $M(\omega, t_0)$. The threshold value of h_{ac} for the onset of the phenomenon, in the cases of the optimal polarization and for linear polarization along each of the coordinate axes, is, respectively,

$$h_{ac, \text{opt}}^{\text{crit}} = \frac{2\alpha\Omega_d}{|\mathbf{u}(\omega)|}, \quad h_{ac, i}^{\text{crit}} = \frac{2\alpha\Omega_d}{|u_i(\omega)|}, \quad (16)$$

where $i = x, y, z$.

We now consider the case when the system is driven by the spin-polarized injected currents alone, i.e., $\mathbf{h}_{ac}(t) = 0$. By using Eqs. (11) and (13), we obtain the Melnikov function

$$\varepsilon M(\omega, t_0) = 2\alpha\Omega_d \pm \beta_{ac} \frac{\pi |\mathbf{e}_p \cdot \mathbf{e}_{d\uparrow}|}{\cosh \frac{\omega\pi}{2\Omega_d}} \cos(\omega t_0 + \delta_p).$$

Hence, the general expression of the threshold for heteroclinic tangle creation is

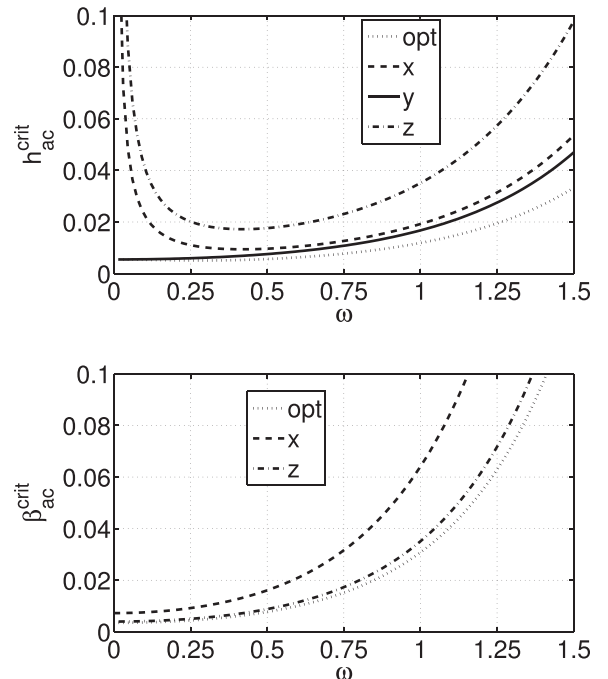


FIG. 2. Threshold values of ac fields and injected currents for creation of heteroclinic tangle versus ω for the various polarizations. Values of the parameters: $\alpha = 0.01$, $D_x = -0.3$, $D_y = 0$, and $D_z = 1$.

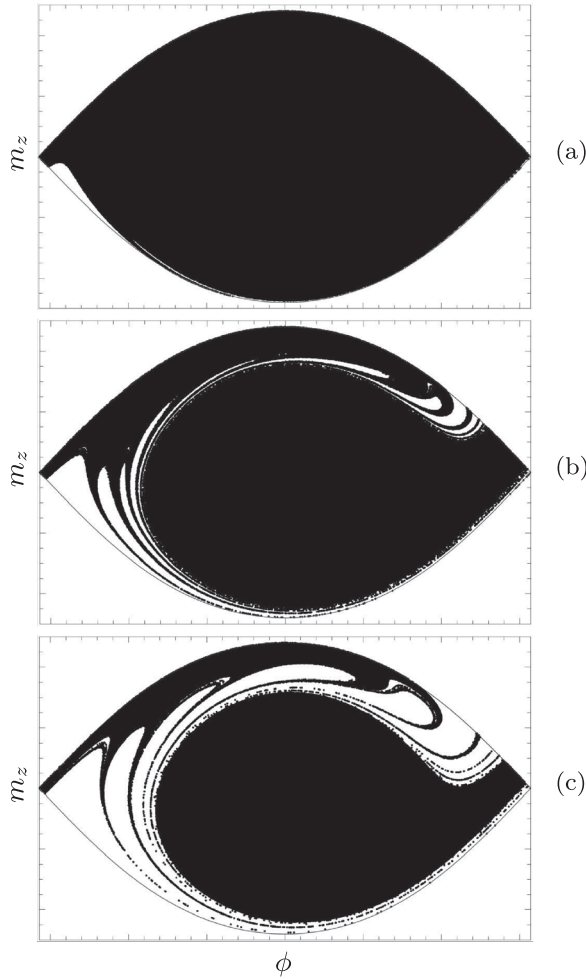


FIG. 3. Basin erosion produced for fields linearly polarised along the y direction: (a) $h_{ay}=0.01$, (b) $h_{ay}=0.015$, and (c) $h_{ay}=0.02$. The figures show the region $-\pi/2 \leq \phi \leq \pi/2$ and $-0.5 \leq m_z \leq 0.5$ of the (m_z, ϕ) -plane. The low energy well is initially filled by 524 288 phase points. When the trajectory originating from a phase point escapes the well within the 20 iterations of the stroboscopic map, it is considered “unsafe” and disregarded. The phase point remaining in the well corresponding to “safe” initial conditions. Values of parameters: $D_x=-0.3$, $D_y=0$, $D_z=1$, $\alpha=0.01$, $\omega=2\pi/16=0.3927$, and $h_{ay}^{\text{crit}}=0.007$.

$$\beta_{ac}^{\text{crit}} = \frac{2\alpha\Omega_d}{\pi|\mathbf{e}_p \cdot \mathbf{e}_{d\uparrow}|} \cosh \frac{\pi\omega}{2\Omega_d}.$$

The optimal (minimum) value is achieved for $\mathbf{e}_p = \pm(k'\mathbf{e}_x + k\mathbf{e}_z)$ or $\mathbf{e}_p = \pm(k'\mathbf{e}_x - k\mathbf{e}_z)$. The former (latter) case correspond to the fact that \mathbf{e}_p is parallel to $\nabla_{\Sigma}g_0$ along the two heteroclinic trajectories which converge towards the saddle point $\mathbf{m} = \mathbf{e}_y$ ($\mathbf{m} = -\mathbf{e}_y$). The threshold corresponding to the optimal polarization and to polarizations along the coordinate axes is, respectively,

$$\beta_{ac,\text{opt}}^{\text{crit}} = \frac{2\alpha\Omega_d}{\pi} \cosh \frac{\pi\omega}{2\Omega_d}, \quad (17)$$

$$\beta_{ac,x}^{\text{crit}} = \beta_{ac,\text{opt}}^{\text{crit}}/k', \quad \beta_{ac,z}^{\text{crit}} = \beta_{ac,\text{opt}}^{\text{crit}}/k, \quad (18)$$

while $\beta_{ac,y}^{\text{crit}} = \infty$. The infinite result for the case of y -polarization is due to the fact that the method is first order accurate in ε . This means that a spin-polarization along the y direction produces a weaker effect with respect to other orientations.

The outcomes of the analytical formulas above are summarized in Fig. 2. This figure shows the threshold of AC fields and injected currents for creation of heteroclinic tangle versus ω , for typical values of the parameters.

A direct consequence arising from the onset of the heteroclinic tangle on the magnetization dynamics is the phenomenon of erosion of the basins of attraction. Such a phenomenon has been studied numerically by solving Eq. (1) for an ensemble of very large number of initial conditions filling the energy well around $\mathbf{m} = +\mathbf{e}_x$. The erosion is illustrated in Fig. 3 which is obtained by progressively removing the points that escape the energy well. The erosion has important practical consequences as it is similar to a reduction of the depth of the potential well and thus it reduces the “safety region” around a stable equilibrium state. In addition to that, the boundary of the basin of attraction of asymptotic regimes inside the well acquires a fractal nature. These phenomena might be at the basis of complex features obtained in the measurement of Stoner-Wohlfarth astroid in the presence of microwave fields.¹¹

It is expected that the phenomena analyzed in this paper may be relevant in the area of spintronic devices when microwave excitations are used to assist the switching of magnetization.¹² In such situations, the behavior of the system near the homoclinic/heteroclinic cycles has a crucial influence on the switching field or on the switching current.^{9,10}

This work was partially supported by MIUR-PRIN Project No. 2010ECA8P3 DyNanoMag and by the National Science Foundation.

¹Nonlinear Phenomena and Chaos in Magnetic Materials, edited by P. E. Wigen (World Scientific Publishing, Singapore, 1994).

²C. Kittel, *Phys. Rev.* **73**, 155 (1948).

³D. J. Seagle, S. H. Charap, and J. O. Artman, *J. Appl. Phys.* **57**, 3706 (1985).

⁴J. M. T. Thompson, *Proc. R. Soc. London, Ser. A* **421**, 195 (1989).

⁵J. Guckenheimer and P. Holmes, *Nonlinear Oscillations, Dynamical Systems, and Bifurcations of Vector Fields* (Springer, New York, 1986).

⁶G. Bertotti, I. D. Mayergoyz, and C. Serpico, *Nonlinear Magnetization Dynamics in Nanosystems* (Elsevier, Amsterdam, 2009).

⁷E. Ott, *Chaos in Dynamical Systems* (Cambridge University Press, Cambridge, 1997).

⁸S. Wiggins, *Introduction to Applied Nonlinear Dynamical Systems and Chaos* (Springer, New York, 1990).

⁹M. d’Aquino, C. Serpico, G. Bertotti, I. D. Mayergoyz, and R. Bonin, *IEEE Trans. Magn.* **45**, 3950–3953 (2009).

¹⁰M. d’Aquino, G. Di Fratta, C. Serpico, G. Bertotti, R. Bonin, and I. D. Mayergoyz, *J. Appl. Phys.* **109**, 07D349 (2011).

¹¹C. Thirion, W. Wernsdorfer, and D. Mailly, *Nat. Mater.* **2**, 524 (2003).

¹²Y.-T. Cui, J. C. Sankey, C. Wang, K. V. Thadani, Z.-P. Li, R. A. Buhrman, and D. C. Ralph, *Phys. Rev. B* **77**, 214440 (2008).